



Short communication

## Pt–Ru–TiO<sub>2</sub> photoelectrocatalysts for methanol oxidation

André S. Polo\*, M.C. Santos, Rodrigo F.B. de Souza, Wendel A. Alves

Centro de Ciências Naturais e Humanas, CCNH, Universidade Federal do ABC – UFABC, Av. dos Estados, 5001, Santo André 09210-170, SP Brazil

### ARTICLE INFO

#### Article history:

Received 22 May 2010

Received in revised form 22 June 2010

Accepted 23 June 2010

Available online 30 June 2010

#### Keywords:

Photoelectrocatalysts

Methanol oxidation

Titanium dioxide

Nanostructures

Electrocatalysis

Photocatalysis

### ABSTRACT

Novel photoelectrocatalysts composed of PtRuTiO<sub>2</sub>/C are prepared by the polymeric precursor method and are characterized by scanning electron microscopy, energy dispersive spectroscopy, transmission electron microscopy and cyclic voltammetry. The onset potential for methanol oxidation is similar (0.3 V vs. RHE) for all of the photoelectrocatalyst layers investigated, although the peak current density is dependent on the layer composition. Irradiation of UV light on the photoelectrocatalyst surfaces enhances the chronoamperometric responses up to 18%, which clearly demonstrates a synergistic effect between the photo- and electrocatalysts. The comparison between all the layers prepared indicates that there is an appropriate ratio of metallic nanoparticles and TiO<sub>2</sub> to obtain the best performance of these photoelectroactive layers. These results demonstrate that methanol oxidation is achieved by electro- and photocatalysis using a simple and affordable method. This procedure can be conveniently exploited to enhance the response of direct methanol fuel cell electrodes.

© 2010 Elsevier B.V. All rights reserved.

### 1. Introduction

Energy is one of the important issues of the 21st century [1,2]. Advances in science and technology have focused on finding new alternatives and approaches to improve energy generation, such as the conversion of sunlight into electricity [3–5] or into high-energy products by processes that mimic photosynthesis [6,7]. Fuel cells have also been exploited for this purpose.

Fuel cells have been known since the middle of the 19th century and have gained great attention during the 1960s because of developments in space technology [8]. Different architectures and fuels have been developed for these devices. Among several options, methanol is a safer and cheaper alternative than the use of hydrogen.

The development of direct methanol fuel cells has the disadvantages of the formation of methanol byproducts and inefficient catalysis. The most efficient electrocatalyst so far is a mixture of platinum and ruthenium, which decomposes methanol and its byproducts by a bifunctional mechanism [9]. Layers of these metals have already been prepared by several methods [10–16]. Methanol can also be photocatalytically oxidized by wide band gap semiconductors. In this case, light excites the semiconductor, which promotes an electron from the valence to the conducting band, and the vacancy created oxidizes the methanol [17].

Electrocatalytical and photocatalytical processes for methanol oxidation can be coupled and the currents produced from both phenomena can be combined. This approach was reported using catalysts supported on carbon fiber [18]. Another approach to join photo- and electrocatalytical processes is the co-sputtering of TiO<sub>2</sub> and platinum particles [19]. In both cases, a better performance was observed under light irradiation.

In this work, new photoelectrocatalyst layers were prepared by the polymeric precursor method. These layers were characterized by electron microscopy and cyclic voltammetry in an acidic medium and their performance for methanol oxidation under UV light were investigated. By adding the methanol photocatalyst, the new materials have the advantage of using lower amounts of electrocatalysts, which can reduce the cost of these materials. Accordingly, these materials offer a more simple and affordable approach for methanol oxidation.

### 2. Experimental

#### 2.1. TiO<sub>2</sub> preparation

Nanocrystalline TiO<sub>2</sub> was prepared as described in the literature [4,20]. Generally, 13 mL of titanium isopropoxide (Strem or Fluka, USA) was slowly added to an acid solution and vigorously stirred (0.5 mL of HNO<sub>3</sub> (Synth, Brazil) in 100 mL of H<sub>2</sub>O) to produce acid hydrolysis of the TiO<sub>2</sub> precursor. The suspension was kept under this condition for 8 h at 50 °C and the resulting solution was then placed in a pressure vessel for 8 h at 200 °C for hydrothermal growth of the nanoparticles. This procedure resulted in TiO<sub>2</sub> particles with a size of ~20 nm.

\* Corresponding author. Tel.: +55 11 4996 0150; fax: +55 11 4996 0090.  
E-mail address: [andre.polo@ufabc.edu.br](mailto:andre.polo@ufabc.edu.br) (A.S. Polo).

**Table 1**

Composition of the prepared photoelectrocatalyst layers.

Layer	%TiO <sub>2</sub>	%Pt	%Ru
A	10	10	0
B	10	5	2.6
C	20	5	2.6
D	0	5	2.6
E	30	5	2.6
F	20	10	5.2
G	10	2.5	1.3

## 2.2. Preparation of photoelectroactive layers

The photoelectroactive layers were prepared using a modified polymeric precursor method [21]. Briefly, polymeric precursors were prepared by mixing metallic salts (H<sub>2</sub>PtCl<sub>6</sub> (Fluka, USA) and/or RuCl<sub>3</sub>·3H<sub>2</sub>O (Riedel, Germany)), citric acid (Aldrich, China) and ethylene glycol, EG (Synth, Brazil), at 60 °C (1:50:300), and the resulting solution was added to an appropriate amount of carbon black (Vulcan XC-72R – Cabot, Brazil). The molar ratio of Pt and Ru was kept at 1, except for a sample in which only platinum was used. For the preparation of the photoelectrocatalysts, TiO<sub>2</sub> was also added to the mixture. The suspensions were homogenized for 1 h in an ultrasonic bath and were thermally treated at 400 °C for 2 h under N<sub>2</sub> atmosphere. The resulting powder was suspended in a mixture of water and Nafion<sup>®</sup>, homogenized for 15 min in an ultrasonic bath and 10 μL of the suspension was then deposited onto a glassy carbon electrode to dry. Different amounts of TiO<sub>2</sub> were added to the mixtures to prepare layers with distinct TiO<sub>2</sub>:Pt nanoparticles layer ratios. The expected compositions of each layer are listed in Table 1.

## 2.3. Electron microscopy

Scanning electron microscopy experiments were carried out on a FEG-SEM (JSM 6330F) or a LV-SEM (JSM 5900LV) microscope (JEOL, Japan). The LV-SEM microscope was equipped with an energy dispersive X-ray detector, which was employed to perform energy dispersive spectroscopy (EDS) experiments. High-resolution transmission electron microscopy experiments were carried out with a HR-TEM (JEM 3010 URP) (JEOL, Japan).

## 2.4. Electrochemical experiments

Electrochemical measurements were performed with a PGSTAT 302N potentiostat/galvanostat (Autolab, The Netherlands). A glassy carbon working electrode was used as a support for the photoelectroactive layers. Platinum and reversible hydrogen electrodes (RHE) were used as auxiliary and reference electrodes, respectively. Milli-Q ultrapurewater was employed in all experiments. The cyclic voltammetric and chronoamperometric measurements were performed in HClO<sub>4</sub> (Carlo Erba, Italy – 0.1 mol L<sup>-1</sup>) in the absence or in the presence of 0.5 or 2.0 mol L<sup>-1</sup> of methanol (Synth, Brazil).

The electrochemical experiments were always carried out under N<sub>2</sub> atmosphere.

## 2.5. Light source

The UV light was provided by a homemade apparatus composed of a high-pressure Hg light bulb from a commercial arc lamp (Philips, Brazil – HPLN 125 W). The exposure onto the electrode surface was manually controlled by a shutter. The surface of the electrodes was irradiated at intervals of 60 s followed by another 60 s in the dark while chronoamperometric experiments were performed. The cycles were repeated up to 600 s.

## 3. Results and discussion

### 3.1. Characterization of photoelectrocatalyst layers

The surface morphology of the prepared photoelectrocatalyst layers was characterized by scanning electron microscopy (SEM). The presence of platinum, ruthenium and titanium dioxide was confirmed by energy dispersive spectroscopy (EDS) experiments and information on the nanoparticles sizes were obtained by high-resolution transmission electron microscopy (HR-TEM). These images are shown in Fig. 1.

The photoelectrocatalyst layers have high surface areas that enhance the performance of the methanol oxidation process. SEM images, as seen in Fig. 1a, confirmed the expected porous and structured surface of the layers. EDS experiments were carried out on all the layers investigated and the spectra obtained were similar to those in Fig. 1b. The EDS exhibited peaks at 2.08, 2.57 and 4.52 keV and were assigned to platinum, ruthenium and titanium, respectively. The signals of carbon and oxygen were also observed at 0.263 and 0.504 keV. This technique confirmed the presence of both electrocatalysts (Pt and/or Ru) and photocatalyst in the composition of the layers.

To evaluate the size of the nanoparticles, HR-TEM was performed because the expected size of the metallic nanoparticles ranged from 3 to 10 nm. The results, shown in Fig. 1c, are in agreement with those reported for similar materials (~6–10 nm) [21,22]. Due to the conditions of the experiment, the TiO<sub>2</sub> nanoparticles did not have enough contrast and were therefore not visible, as shown in Fig. 1c. These particles have a diameter of ~20 nm. The presence of TiO<sub>2</sub> on the layers was confirmed by EDS experiments.

The layers were also evaluated by their electrochemical response in acidic medium, as seen in Fig. 2. In Fig. 2 inset, a voltammetric profile for photoelectrocatalyst layers A and B are shown with fair resolution of the platinum features. These features include hydrogen UPD adsorption/desorption as well as formation and reduction of PtO, as discussed in the literature for Pt/C dispersed catalysts [23,24]. Layer B presents typically higher capacitive currents in comparison to layer A, due to the charging processes of RuO<sub>2</sub> [22,25,26].

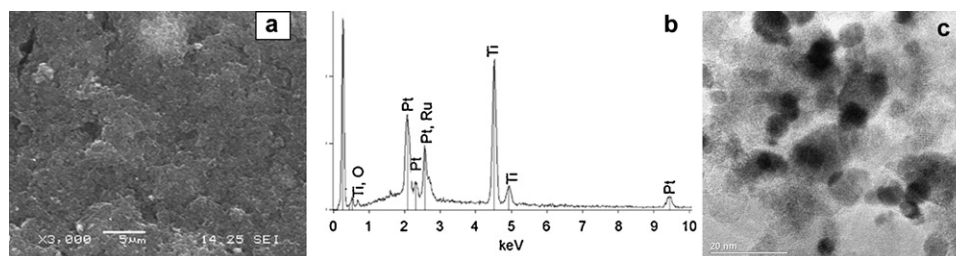


**Fig. 1.** Electron microscopy experiments for characterization of layer B. SEM image (a) and EDS analysis (b) of the layer B and HR-TEM image (c) of the powder prepared.

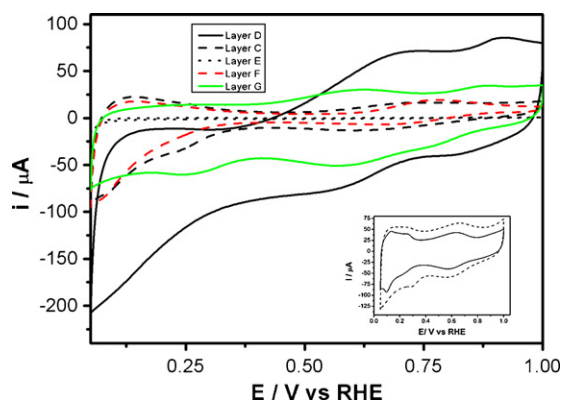


Fig. 2. Cyclic voltammograms for the photoelectroactive layers prepared in acidic medium ( $\nu = 10 \text{ mV s}^{-1}$ ;  $[\text{HClO}_4] = 0.1 \text{ mol L}^{-1}$ ). Inset: cyclic voltammograms for the photoelectroactive layers A (---) and B (- - -), under the same conditions.

By comparing the layers that have the same amount of electrocatalyst and different percentages of  $\text{TiO}_2$  (e.g., layers C–E), it can be concluded that layers with more  $\text{TiO}_2$  have lower capacitive current. For these layers, the voltammetric profiles were not as sharp and defined as it was for a clean Pt electrode (or for  $\text{TiO}_2$  having platinum catalyst on its surface) in sulfuric acid [27].

### 3.2. Methanol oxidation

Most of the photoelectroactive layers, which were prepared in the presence of  $0.5 \text{ mol L}^{-1}$  of methanol, exhibited cyclic voltammograms similar to the electrocatalyst layers already described for methanol oxidation [23,25], as seen in Fig. 3.

The onset potential for methanol oxidation was observed in the range of 0.3–0.4 V, which is in accordance with the Pt/C electrocatalysts used for the same process [23]. The photoelectrocatalyst layers also exhibited an oxidation peak ( $E_{\text{pOx}}$ ) on the forward scan and another oxidation peak on the reverse scan. The onset potential and both  $E_{\text{pOx}}$  are listed in Table 2 for all the layers investigated.

The oxidation peaks of the forward scan were close to the values previously reported [23,25] and were attributed to the oxidation of methanol byproducts, which were strongly adsorbed onto the catalyst surface [28]. The peak observed during the reverse scan was probably due to the reactivation of the Pt nanoparticles surface, followed by the oxidation of methanol or its residues.

An interesting observation was that layer D, which did not have  $\text{TiO}_2$  in its composition, did not present an oxidation peak. How-

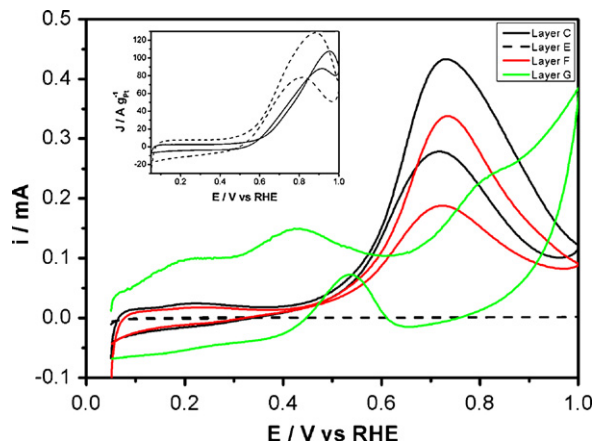


Fig. 3. Cyclic voltammograms of the prepared photoelectroactive layers. Inset: cyclic voltammograms of photoelectroactive layers A (---) and B (- - -). ( $\nu = 10 \text{ mV s}^{-1}$ ;  $[\text{MeOH}] = 0.5 \text{ mol L}^{-1}$ ;  $[\text{HClO}_4] = 0.1 \text{ mol L}^{-1}$ ).

Table 2

Electrochemical parameters of methanol oxidation determined for each photoelectrocatalyst layer prepared.

Layer	Onset potential, V	$E_{\text{pOx}}$ , V	
		Fwd	Rev
A	0.32	0.95	0.93
B	0.32	0.88	0.81
C	0.38	0.73	0.72
D	–	–	–
E	–	–	–
F	0.38	0.73	0.72
G	–	–	–

ever, layer E, which had the highest  $\text{TiO}_2$  content among the layers with 5% of platinum, also did not exhibit an oxidation peak. These observations suggest that an optimal ratio exists between photo- and electrocatalyst, in which their cooperative effect would result in the best performance. The behavior observed for layer G, which also had a high content of  $\text{TiO}_2$  relative to the content of electrocatalysts, corroborates this hypothesis.

Chronoamperometric experiments were carried out at 0.5 V because there is no practical importance above this potential. An abrupt current decrease was observed for the photoelectrocatalyst layers as the UV light was blocked, and there was an abrupt growth as the shutter was opened. Layer B exhibited current density higher than layer A throughout the experiment. The comparison between layers A and B, shown in Fig. 4 inset, indicates an improved performance for the layer that had ruthenium nanoparticles present in its composition.

The higher efficiency of layer B in comparison to layer A is due to the bifunctional mechanism [11], which consists of the adsorption of the fuel onto catalyst sites and, after several successive electron transfer steps, results in the adsorbed intermediate  $\text{CO}_{\text{ads}}$  (Eq. (1) [28]).



The  $\text{CO}_{\text{ads}}$  reacts with the OH adsorbed,  $\text{OH}_{\text{ads}}$ , to yield  $\text{CO}_2$ , Eq. (2). This is the determining step of the overall reaction rate, under steady state conditions.



To enhance the effect, it was found that the final step occurred by reaction of  $\text{CO}_{\text{ads}}$  at Pt and  $\text{OH}_{\text{ads}}$  at ruthenium

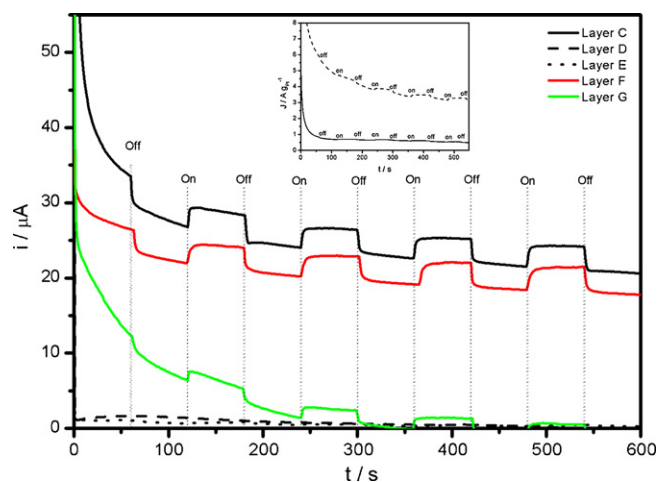


Fig. 4. Chronoamperometry for oxidation of methanol under UV light of prepared photoelectroactive layers. ( $E = 0.5 \text{ V}$  vs. RHE). Inset: chronoamperometry for layers A (---) and B (- - -);  $[\text{MeOH}] = 2.0 \text{ mol L}^{-1}$ ;  $[\text{HClO}_4] = 0.1 \text{ mol L}^{-1}$ .

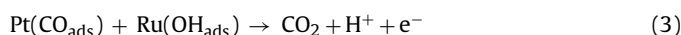
**Table 3**

Current of the photoelectrocatalyst layers under UV irradiation and percentage increase in current.

Layer	<i>i</i> , mA	Increase
C	23.9	13%
D	0.31 <sup>a</sup>	–
E	0.32	3%
F	21.4	18%
G	0.3	–

<sup>a</sup> Values determined in the dark since there is no photocatalyst.

surfaces [28], Eq. (3).



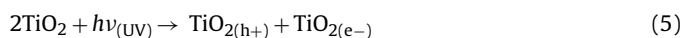
The mechanisms presented explain the behavior of the layers. The area of the cyclic voltammogram of layer B was wider than layer A, which indicated a higher amount of charge was involved in the oxidation process. Layer A had only platinum as the electrocatalyst, which could be easily poisoned by the intermediates of the oxidation process and consequently could reduce the electrode performance. The presence of ruthenium in the layer improved the anodic currents, depoisoning the electrode by the oxidation of byproducts through the bifunctional mechanism, as described by Eqs. (1)–(3).

The existence of the bifunctional mechanism facilitated the completion of methanol oxidation and reduced the potential of the process. Because the presence of ruthenium nanoparticles improved the performance, all the others layers were prepared with a mixture of platinum and ruthenium nanoparticles with a 1:1 molar ratio.

In addition to electro-oxidation, the methanol photo-oxidation also contributed to a better performance of the electrodes under UV irradiation. Irradiation of UV light onto photoelectrocatalysts surfaces improved the performance of the electrodes in comparison to their dark current. The percentage increase of the current of these photoelectrocatalyst layers was determined by subtracting the value of the current under light irradiation at 540 s ( $i_{540\text{s}}$ ) by the current in the dark at 550 s ( $i_{550\text{s}}$ ). The result was then divided by  $i_{550\text{s}}$  and multiplied by 100% as demonstrated in Eq. (4). The percentage increases determined by this way are listed in Table 3.

$$\text{increase \%} = \frac{i_{540\text{s}} - i_{550\text{s}}}{i_{550\text{s}}} \times 100\% \quad (4)$$

The incidence of UV light on the photoelectroactive layers promoted methanol photo-oxidation. Irradiation of TiO<sub>2</sub> by UV light promoted the electron from the valence band to the conducting band. Consequently, an electron-hole pair was created (Eq. (5)) and the methanol was oxidized by TiO<sub>2(h+)</sub> [29,30].



The irradiation of TiO<sub>2</sub> could have enhanced the performance of the layers in two different ways. The hole, h<sup>+</sup>, created after the light irradiation of the compound could be capable of oxidizing methanol molecules. In addition to this effect, the electron on the conducting band improved the conductivity of the layer and enhanced the performance of the bimetallic catalysts on the electro-oxidation of the methanol [30]. The synergy between photo- and electrocatalysis of methanol improved up to 18% of the current of the photoelectroactive layers exposed to the light. These results are listed in Table 3.

One possible explanation for the cooperation between the electro- and photocatalysis processes is related to the mechanisms involved. In the dark, the current observed was due to the methanol electro-oxidation promoted by platinum and/or ruthenium catalyst sites. Upon UV irradiation, the photo-oxidation mechanism contributed to the overall current. The hole created in the valence band

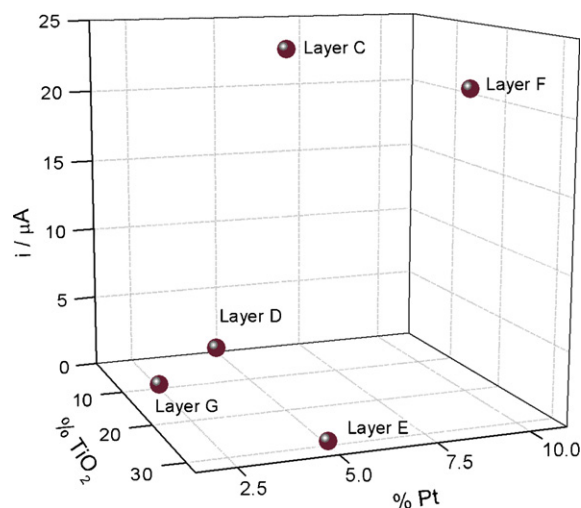


**Fig. 5.** Composition and anodic current determined under irradiation and 0.5 V for layer C–G.

was capable of accepting an electron from the methanol and oxidized it. The photo-oxidation of methanol was already known [18] and the improvement of the anodic current was ascribed to the electronic population of the conducting band. Because methanol was oxidized by reducing the valence band, the photocatalyst was not degraded.

The relationship of the photoelectrocatalyst layers composition and their performances in methanol oxidation were evaluated by their anodic current at 0.5 V and under UV irradiation. These data are depicted in Fig. 5.

Higher anodic currents were observed for layers C and F, which had 20% TiO<sub>2</sub>. This amount of photocatalyst seemed to be the best for photoelectroactive layers. Even more interesting was that layer C performed better than layer G, even though it had less ruthenium and platinum. This fact can lead to the preparation of photoanodes for direct methanol fuel cells at lower costs because less noble metals are necessary for their construction.

Further investigations on changing the amount of electrocatalyst to improve the performance of the layer are worth pursuing.

#### 4. Conclusion

In this work, the polymeric precursor method was employed to prepare new photoelectrocatalyst layers for methanol oxidation, which were characterized by SEM, EDS and TEM as well as by their cyclic voltammograms in acidic medium. The cyclic voltammetry in the presence of methanol indicated the capacity of the layers to oxidize the alcohol. Chronoamperometric experiments, which were carried out at 0.5 V under UV light, showed an improved performance of the anodic current of up to 18% in comparison to the performance in the dark. This improvement was ascribed to methanol photo-oxidation. A synergistic effect between the photo- and electrocatalysts was also demonstrated. The photoelectrocatalyst with a composition of 20% TiO<sub>2</sub>, 5% Pt and 5% Ru showed the best performance and an increase in noble metals did not improve efficiency. Thus, minimizing the amount of noble metals can be a way to reduce the costs of these layers. The synergy between the photo and electrocatalysts can be conveniently employed to enhance the performance of direct methanol fuel cells.

#### Acknowledgments

The authors are grateful to UFABC, FAPESP (Grants 05/59992-6, 08/53576-9, 09/09145-6) and CNPq (Grant 577256/2008-4,

474732/2008-8) for the financial support as well as LME/LNLS (Brazilian Synchrotron Light Laboratory) for the use of microscopy facilities.

## References

- [1] N. Armaroli, V. Balzani, *Angew. Chem. Int. Ed. Engl.* 46 (2007) 52–66.
- [2] P.V. Kamat, *J. Phys. Chem. C* 111 (2007) 2834–2860.
- [3] M. Grätzel, *Prog. Photovolt. Res. Appl.* 14 (2006) 429–442.
- [4] A.S. Polo, N.Y. Murakami Iha, *Sol. Energy Mater. Sol. Cells* 90 (2006) 1936–1944.
- [5] A.S. Polo, M.K. Itokazu, N.Y. Murakami Iha, *Coord. Chem. Rev.* 248 (2004) 1343–1361.
- [6] J.H. Alstrum-Acevedo, M.K. Brennaman, T.J. Meyer, *Inorg. Chem.* 44 (2005) 6802–6827.
- [7] L.A. Silva, S.Y. Ryu, J. Choi, W. Choi, M.R. Hoffmann, *J. Phys. Chem. C* 112 (2008) 12069–12073.
- [8] L. Carrette, K.A. Friedrich, U. Stimming, *Chem. Phys. Chem.* 1 (2000) 162–193.
- [9] S. Wasmus, A. Küver, *J. Electroanal. Chem.* 461 (1999) 14–31.
- [10] J.C. Davies, B.E. Hayden, D.J. Pegg, *Surf. Sci.* 467 (2000) 118–130.
- [11] J.C. Davies, B.E. Hayden, D.J. Pegg, M.E. Rendall, *Surf. Sci.* 496 (2002) 110–120.
- [12] L. Dubau, C. Coutanceau, E. Garnier, J.M. Leger, C. Lamy, *J. Appl. Electrochem.* 33 (2003) 419–429.
- [13] Z. Jusys, J. Kaiser, R.J. Behm, *Electrochim. Acta* 47 (2002) 3693–3706.
- [14] Z.D. Wei, L.L. Li, Y.H. Luo, C. Yan, C.X. Sun, G.Z. Yin, P.K. Shen, *J. Phys. Chem. B* 110 (2006) 26055–26061.
- [15] J. Croy, S. Mostafa, H. Heinrich, B. Cuenya, *Catal. Lett.* 131 (2009) 21–32.
- [16] Q.-Z. Jiang, X. Wu, M. Shen, Z.-F. Ma, X.-Y. Zhu, *Catal. Lett.* 124 (2008) 434–438.
- [17] B. Ohtani, S. Nishimoto, *J. Phys. Chem.* 97 (1993) 920–926.
- [18] K. Drew, G. Girishkumar, K. Vinodgopal, P.V. Kamat, *J. Phys. Chem. B* 109 (2005) 11851–11857.
- [19] K.-W. Park, S.-B. Han, J.-M. Lee, *Electrochem. Commun.* 9 (2007) 1578–1581.
- [20] C.G. Garcia, A.S. Polo, N.Y. Murakami Iha, *J. Photochem. Photobiol. A* 160 (2003) 87–91.
- [21] R.G. Freitas, L.F. Marchesi, R.T.S. Oliveira, F.I. Mattos-Costa, E.C. Pereira, L.O.S. Bulhoes, M.C. Santos, *J. Power Sources* 171 (2007) 373–380.
- [22] M.C. Santos, L. Cogo, S.T. Tanimoto, M.L. Calegari, L.O.S. Bulhões, *Appl. Surf. Sci.* 253 (2006) 1817–1822.
- [23] J.W. Guo, T.S. Zhao, J. Prabhuram, C.W. Wong, *Electrochim. Acta* 50 (2005) 1973–1983.
- [24] E.V. Spinacé, A.O. Neto, T.R.R. Vasconcelos, M. Linardi, *J. Power Sources* 137 (2004) 17–23.
- [25] L.P.R. Profeti, F.C. Simões, P. Olivi, K.B. Kokoh, C. Coutanceau, J.M. Léger, C. Lamy, *J. Power Sources* 158 (2006) 1195–1201.
- [26] M.C. Santos, A.J. Terezo, V.C. Fernandes, E.C. Pereira, L.O.S. Bulhoes, *J. Solid State Electrochem.* 9 (2005) 91–95.
- [27] B.E. Hayden, D.V. Malevich, D. Pletcher, *Electrochem. Commun.* 3 (2001) 395–399.
- [28] T. Iwasita, *Electrochim. Acta* 47 (2002) 3663–3674.
- [29] M. Miyake, H. Yoneyama, H. Tamura, *J. Catal.* 58 (1979) 22–27.
- [30] J.M. Macak, P.J. Barczuk, H. Tsuchiya, M.Z. Nowakowska, A. Ghicov, M. Chojak, S. Bauer, S. Virtanen, P.J. Kulesza, P. Schmuki, *Electrochem. Commun.* 7 (2005) 1417–1422.